Desalination and Water Treatment
www.deswater.com

doi: 10.5004/dwt.2017.0300

62 (2017) 377–386
February

Kinetic and equilibrium studies of chromium (VI) metal ions adsorption using Amberlite IRA-420 anions exchanger

M.S. Mohy Eldin[a,b,*], Khalid A. Alamry[c], Z.A. Khan[a], A.E.M. Mekky[a,d], T.S. Saleh[a,e]

[a]*Chemistry Department, Faculty of Science, University of Jeddah, Asfan P.O. Box 80203, Jeddah 21589, Saudi Arabia, Tel. +966 569006640; emails: m.mohyeldin@mucsat.sci.eg (M.S. Mohy Eldin), ziyaakhan@gmail.com (Z.A. Khan), ataher2211@yahoo.com (E.M. Mekky), tamsaid@yahoo.com (T.S. Saleh)*
[b]*Polymer Materials Research Department, Advanced Technology, and New Materials Research Institute, SRTAC, New Borg El-Arab City 21934, Alexandria, Egypt*
[c]*Chemistry Department, Faculty of Science, King Abdul Aziz University, Jeddah 21589, Saudi Arabia, email: kaalamri@kau.edu.sa*
[d]*Chemistry Department, Faculty of Science, Cairo University, Giza, Egypt*
[e]*Green Chemistry Department, National Research Centre, Dokki, Cairo 12622, Egypt*

Received 17 March 2017; Accepted 16 July 2016

ABSTRACT

A fundamental investigation of the removal of chromium (VI) ions ($HCrO_4^-$ and $Cr_2O_7^{2-}$) from aqueous solutions by Amberlite IRA-420 anions exchanger particles (AMB) was conducted under batch conditions. The kinetic and equilibrium results obtained for chromium (VI) ions sorption with different initial concentrations onto AMB were analyzed. Kinetic modeling analysis with three different types of kinetic sorption models (pseudo-first-order, pseudo-second-order, and simple Elovich models) was applied to simulate the chromium (VI) ions sorption data. The analysis of the kinetic data indicated that the sorption was a second-order process. An ion-exchange mechanism may have existed in the chromium (VI) ions sorption process with AMB. The chromium (VI) ions uptake by AMB was quantitatively evaluated with equilibrium sorption isotherms. The experimental data of the removal equilibrium were correlated with the Langmuir, Dubinin–Radushkevich (D–R), Freundlich, and Harkins-Jura isotherm models, and the applicability of these isotherm equations to the sorption systems was compared by the correlation coefficients.

Moreover, diffusion mechanism of chromium (VI) ions was described by different adsorption diffusion models. The diffusion equations inside particulate of Dumwald–Wagner and intraparticle models were used to calculate the diffusion rate. The actual rate-controlling step involved in the chromium (VI) ions sorption process was determined by further analysis of the sorption data by the kinetic expression given by Boyd.

Keywords: Anions exchanger; Adsorption; Chromium (VI) metal ions; $HCrO_4^-$ and $Cr_2O_7^{2-}$; Removal; Kinetics; Equilibrium; Diffusion; Models

1. Introduction

Water pollution is becoming a major problem endangering all living beings. This issue is not only currently acute but also becoming regressive day by day. The effects of water pollution strongly impact the gentle balance of nature. The pollutants of water are classified as organic and inorganic pollutants. The inorganic pollutants consist mainly the heavy metals (metallic elements). Metals and metalloids due to their extensive use represent a significant fraction of the contaminants [1]. Heavy metals like iron, manganese, lead, mercury, chromium, cadmium, nickel, cobalt, beryllium and copper are present in both natural and contaminated environments. They act as the minerals when they are found within the permissible limits. In well-balanced natural environments, they occur at low concentrations. However, these are present at high levels as is the case

* Corresponding author.

in contaminated environments. They occur naturally as ions, compounds and complexes (speciation) in the environment in a variety of forms [2]. Chromium is one of the toxic element, which is first to remove. Chromium (Cr(VI)) does not occur in nature but is present in ores, primarily in the form of chromite. Chromium exists in two oxidation states, Cr(III) and Cr(VI). Chromium at higher levels is toxic to both man and animals but plays a significant role in glucose and cholesterol metabolism and as an essential element. The hexavalent form is 500 times more toxic to aquatic life than trivalent one [3]. Toxic chromium salts are extensively used in various industries such as leather industry metallurgical industries and in the manufacturing of paints, inks, wood preservatives, photographic materials, textile, rubber, ceramics and fungicides [4–7]. The effluents of these industries having have to be treated for the complete removal of chromium ions before they are discharged into the environment. If rigorous scientific methods of disposal are not followed, there arises a potential danger of entrance of chromium ion into the nearby water bodies. The chromium ions being nondegradable in nature enter into the biological systems and get accumulated in the food chains in unspecific compounds inside the cells of living organisms causing the significant threat to aquatic life [6–9]. Methodologies have been developed in controlling chromium, based on chemical reduction [8,10–12], flocculation [10], electrolysis and electroplating [13,14], nanofiltration [15], bioaccumulation [16], ion exchange [17], adsorption on silica composites [18,19], activated carbons [20–22], fly ash [23], modified zeolites [24,25], bone charcoal [26] and microbes [27]. Some patents are also found in the literature [28].

The aim of this work is to study the kinetic and equilibrium results obtained from chromium (VI) ions sorption with different initial concentrations onto Amberlite IRA-420 anions exchanger particles (AMB) under batch conditions.

2. Materials and methods

2.1. Materials

Amberlite (IRA 420): A commercial Amberlite IRA-420 ion exchange resin supplied by Rohm and Hass (Philadelphia, Pennsylvania, USA) was used.

Potassium dichromate ($K_2Cr_2O_7$), minimum assay 99%, was supplied by Sigma-Aldrich, Germany. Sodium hydroxide (NaOH), minimum assay 99%, was supplied by Sigma-Aldrich, Germany. Sodium chloride (NaCl), minimum assay 99%, was supplied by Sigma-Aldrich, Germany.

2.2. Batch adsorption experiment

The Cr(VI) ions adsorption studies performed by mixing 0.2 g of wet Amberlite IRA 420 (4 g/L) with 50 mL of Cr(VI) ions solution of a particular concentration. The mixture was agitated (300 rpm) using magnetic stirrer for 60 min at room temperature then left to settle for 1 min. The Cr(VI) ions concentration was determined by measuring the absorbance at the maximum wavelength (λ_{max} = 380 nm) using UV-VIS spectrophotometer and multiply by 156.25 constant.

The adsorption process characterized by two parameters namely the removal percentage (%) and the adsorption capacity (mg/g).

The removal percentage is calculated according to the following formula:

$$\text{Cr(VI) ions removal (\%)} = [(C_0 - C_t) / C_0] \times 100 \quad (1)$$

The adsorption capacity is calculated according to the following formula:

$$q\ (\text{mg/g}) = V\,(C_0 - C_t) / M \quad (2)$$

where C_0 and C_t (mg L^{-1}) are the initial at zero time and the final concentration of Cr(VI) ions at a specific time, respectively. q is the uptake capacity (mg/g); V is the volume of the Cr(VI) ions solution (mL); and M is the mass of the AMB (g).

2.3. Sorption kinetic models

The kinetic models were used to follow up the adsorption rate of the process. Three frequently used kinetics models, namely the pseudo-first-order, the pseudo-second-order, and finally, the Elovich model, were used in our study.

2.3.1. Pseudo-first-order model

Lagergren and Svenska [29] correlated the adsorption rate to the adsorption capacity to follow up the kinetic of the adsorption process from solution onto solid surface using the following linear equation:

$$\text{Ln}\,(q_e - q_t) = \text{Ln}\,q_e - k_1\,t \quad (3)$$

The pseudo-first-order reaction rate constant k_1 (min^{-1}) obtained from the slope of the linear line is resulted from plotting Ln ($q_e - q_t$) vs. time. The adsorbed amounts (mg/g) at time t (min) are defined as q_t and q_e at equilibrium.

2.3.2. Pseudo-second-order model

The pseudo-second-order model describes the kinetic of the chemisorption process using the following linear form equation [30]:

$$t/q_t = (1/k_2\,q_e^2) + t/q_e \quad (4)$$

The pseudo-second-order reaction rate constants k^2 (g/mg min) and q_e values are determined from the slope and intercept of the plot of t/q_t against time (min).

2.3.3. Elovich model

Despite the routine use of the simple Elovich model in describing the kinetics of chemisorption of gas onto solid systems, it has also been utilized in the recent times to monitor the pollutants adsorption from aqueous solutions. The simple form equation of the Elovich model is as follows [31]:

$$q_t = \alpha + \beta\ \text{Ln}\ t \quad (5)$$

Linear relationship normally obtained by plotting q_t vs. Ln t where the slope and the intercept of the obtained line expressed the initial sorption rate (α, mg/g min), and the extent of surface coverage and activation energy for chemisorption (β, g/mg).

2.4. Sorption mechanisms

2.4.1. Dumwald–Wagner model

The Dumwald–Wagner model describes the diffusion of adsorbate inside particulate by the following equation [32]:

$$\text{Ln}\,(1 - F^2) = -(K/2.303) * t \quad (6)$$

Plotting Ln $(1 - F^2)$ vs. t resulted in a straight line. The diffusion rate constant is K, and the adsorption percent is F, which is calculated by (q_t/q_e).

2.4.2. Intraparticle model

The identification of the adsorption mechanism usually needs to use the intraparticle model [33]:

$$q_t = k_d\, t^{1/2} + C \quad (7)$$

Plotting the adsorption capacity q_t against $t^{1/2}$ normally gives two portion lines. From the second portion line, the intraparticle diffusion rate (k_d) and the thickness of the boundary layer (C) were calculated from the slope and the intercept of the linear portion, respectively.

2.4.3. Boyd model

Boyd et al. identify the rate-controlling step involved in the adsorption step using the following equations [34].

$$F = 1 - (6/\pi^2) \exp(-B_t) \quad (8)$$

The percentage of solute adsorbed at time t (F) is given by the following equation:

$$F = q / q_\alpha \quad (9)$$

The amount of adsorbed solute (mg/g) at any time t and at an infinite time are defined as q and q_α.

B_t is a mathematical function of F and can be calculated for each value of F using Eq. (10) obtaining from substituting Eq. (8) into Eq. (9). Plotting B_t values vs. time giving a straight line which provides useful information to distinguish between external-transport- and intraparticle-transport-controlled rates of sorption.

$$B_t = -0.4978 - \text{Ln}\,(1 - q/q_\alpha) \quad (10)$$

2.5. Sorption isotherm models

The sorption isotherm models deal with the main factors affecting the interaction between the adsorbent surface and the adsorbate. These factors could be mentioned as:

- the homogeneity of the adsorption sites distribution,
- the limitation of adsorption levels (layers) onto the adsorbent surface and inside its pores, and
- the indirect adsorbent/adsorbate interactions.

2.5.1. Langmuir isotherm

The Langmuir isotherm model postulated the formation of monolayer adsorbate onto an entirely homogeneous distribution of adsorption sites onto the adsorbent surface neglecting the interaction between the adsorbate molecules [35].

$$C_e/q_e = 1/q_m\, K + C_e/q_m \quad (11)$$

Plotting of C_e/q_e against C_e presents a straight line of slope $1/q_m$ and intercept $1/q_m\, K$. The Langmuir constants, the maximum adsorption capacity q_m (monolayer capacity; mg/g) and the energy of adsorption K (L/mg), can be calculated from the slope and the intercept, respectively.

To predict the favorableness of the adsorption system, a dimensionless separation factor (R_L) was calculated (Eq. (12)) to identify the isotherm shape [36].

$$R_L = 1/1 + K\, C_0 \quad (12)$$

where C_0 is defined as the cadmium ions initial concentration (mg/L).

2.5.2. Freundlich isotherm

The Freundlich isotherm model, the oldest one, assumed the heterogeneity of the adsorbent surface and the formation of multilayer adsorbate [37]. The linear for of the model is expressed as follows:

$$\text{Ln}\, q_e = \text{Ln}\, K_F + (1/n_f)\, \text{Ln}\, C_e \quad (13)$$

Plotting Ln q_e vs. Ln C_e gives a straight line with a slope $1/n_f$ and an intercept Ln K_F. The q_e is defined as the amount of ions sorbed at equilibrium (mg/g). The adsorbate concentration at equilibrium is C_e (mg/L). The K_F is an indicator of the adsorption capacity, and n_f is an indicator of the adsorption effectiveness.

2.5.3. D–R isotherm

For describing the adsorption of single solute systems, the Dubinin–Radushkevich (D–R) isotherm is usually used. The D–R isotherm on one hand considers the formation of monolayer adsorbate as the Langmuir isotherm, but on the other hand considers the heterogeneity of the adsorbent surface and unequal adsorption potential as the Freundlich isotherm model [38]. It is assumed that the characteristic of the sorption curve is related to the porosity of the adsorbent. The D–R isotherm model linear expression is as follows:

$$\text{Ln}\, q_e = \text{Ln}\, V'_m - K'\varepsilon^2 \quad (14)$$

where q_e is the adsorption capacity at equilibrium (mg/g); V'_m is the D–R maximum sorption capacity (mg/g); K' is the adsorption energy constant (mol^2/kJ^2); and ε is the Polanyi potential.

$$\varepsilon = RT\,(1 + 1/C_e) \quad (15)$$

where R is defined as the gas constant (8.314×10^{-3} kJ/mol K), and T is the temperature (K). The K' is the energy required to transfer of adsorbate molecules from the solution phase to the surface of the solid phase. The nature of the adsorption process, physical or chemical features, extracted from the energy value [39] is calculated according to the following equation [40]:

$$E = (2K')^{-0.5} \quad (16)$$

2.5.4. Harkins-Jura isotherm

The Harkins-Jura adsorption isotherm can be expressed as follows [41,42].

$$1/q_e^2 = (B_H/A_H) - (1/A_H) \text{ Ln } C_e \quad (17)$$

where B_H (mg²/L) and A_H (g²/L) are the isotherm constants. The Harkins-Jura adsorption isotherm accounts to multilayer adsorption and can be explained with the existence of heterogeneous pore distribution. The value of $1/q_e^2$ was plotted against Ln C_e.

3. Results and discussion

The sorption process of Cr(VI) ions is dependent on pH of the equilibrium solution. The hexavalent chromium exists primarily as chromic acid (H_2CrO_4) and its salts, hydrogen chromate ($HCrO_4^-$) and chromate (CrO_4^{2-}) ions depending on the sample pH [43]. The dichromate ion ($Cr_2O_7^{2-}$) is formed when the concentration of chromium exceeds approximately 1 g/L. In the solution, in the whole range of concentrations and when pH > 6.5, only CrO_4^{2-} ions exist. In the pH range from 0 to 6.5, $HCrO_4^-$ and $Cr_2O_7^{2-}$ ions are predominant [44]. A sorption process between a strong base anion exchange resin with quaternary ammonium $-N^+(CH_3)_3$ and chromates from the aqueous solution can be described according to the following reactions [45]:

$$RCl + HCrO^{-4} \rightarrow R - HCrO_4 + Cl^- \quad (18)$$

$$2RCl + CrO_4^{2-} \rightarrow R_2CrO_4 + 2Cl^- \quad (19)$$

$$2RCl + 2HCrO_4^- \rightarrow R_2Cr_2O_7 + 2Cl^- + H_2O \quad (20)$$

$$2RCl + Cr_2O_7^{-2} \rightarrow R_2Cr_2O_7 + 2Cl^- \quad (21)$$

There are two principal means by which anion exchanger and ions can interact with each other in aqueous solutions. The most common way involves ion exchange or chelation of metal ions. These interactions are characterized by the resin structure regarding present functional groups. Amine groups bound to carbon are considered to be the reaction partner of Cr(VI) ions.

Adsorption of chromium (VI) ions from initial metal ions solutions with different concentrations ranged between 300 and 1,000 (mg/L) investigated, and both the removal percentage (%) and the adsorption capacity (mg/g) were calculated and presented in Fig. 1. From the figure, it is evident that the removal percentage was almost constant (95%–97%) while the adsorption capacity linearly increased (Fig. 1). The highest adsorption capacity obtained using 1,000 (mg/L) Cr(VI) ions solution was found around 240 (mg/g).

3.1. Sorption kinetic models

The kinetic study is important for an adsorption process because it depicts the uptake rate of the adsorbate and controls the residual time of the whole adsorption process. Therefore, three different kinetic models, pseudo-first-order, pseudo-second-order and Elovich, were selected in this study for describing the Cr(VI) ions sorption process using AMB.

3.1.1. Pseudo-first-order model

The pseudo-first-order kinetic model was the earliest model about the adsorption rate based on the adsorption capacity. The values of the pseudo-first-order constant k_1 and correlation coefficient, R^2, obtained from the slope of the plot Ln $(q_e - q_t)$ vs. time in Fig. 2 are tabulated in Table 1. From

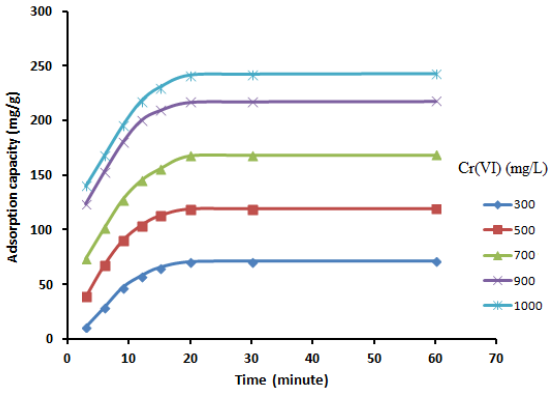

Fig. 1. Effect of the contact time on the removal percentage (%) and adsorption capacity for different chromium (VI) ions concentrations.

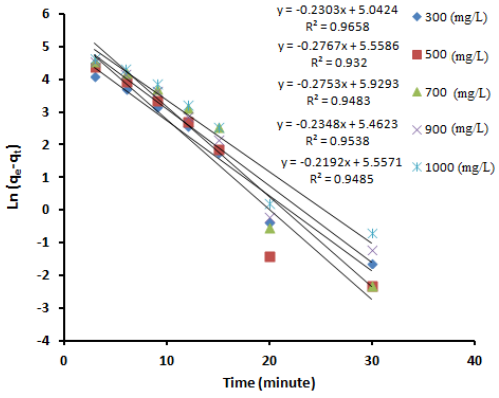

Fig. 2. First-order plot for chromium (VI) ions removal using AMB.

Table 1
The values of the pseudo-first-order constants

Cr(VI) (mg/L)	R^2	$q_{(calc)}$	$q_{(exp)}$	K_1
300	0.9658	155	71.2	0.2303
500	0.932	259.46	119	0.2767
700	0.9483	375.9	168.6	0.2753
900	0.9538	235.64	217.8	0.2348
1,000	0.9485	259	242.5	0.2192

Table 1, it indicated that the correlation coefficients are good enough. However, the estimated values of q_e calculated from the equation have differed from the experimental values especially at the low concentrations, which show that the model is appropriate only to describe the sorption process at high concentrations above 900 (mg/L) (Table 1).

3.1.2. Pseudo-second-order model

The chemisorption kinetics can also be given by the pseudo-second-order model. The pseudo-second-order kinetics applies to the experimental data. The plot of t/q_t vs. t gave a linear relationship as illustrated in Fig. 3. From the figure, the values of q_e calculated and k_2 can be determined from the slope and intercept of the plot, respectively (Table 2). Also, the value of the correlation coefficients, R^2 (1), was extracted. Based on linear regression ($R^2 \approx 1$) values, the kinetics of Cr(VI) ions sorption on to AMB can be described well by the second-order equation. That suggests that the rate-limiting step in these sorption processes may be chemisorptions involving valent forces through the sharing or exchanging of electrons between sorbent and sorbate [46]. Additionally, comparing the values of q_e calculated resulted from the intersection point of the second-degree reaction kinetic curve with that obtained from the experimental data. Thus, second-order rate expression fits the data most satisfactorily.

3.1.3. Elovich model

The simple Elovich model is one of the most useful models for describing the kinetics of chemisorption of gas onto solid systems. However, recently, it has also been applied to describe the adsorption process of pollutants from aqueous solutions. Fig. 4 illustrates the plot of q_t against Ln t for the sorption of Cr(VI) ions onto AMB. From the slope and intercept of the linearization of the simple Elovich equation, the estimated Elovich equation parameters were obtained (Table 3). The values of β are indicative of the number of sites available for adsorption while α values are the adsorption quantity when Ln t is equal to zero, i.e., the adsorption quantity when t is 1 h. This value is helpful in understanding the adsorption behavior of the first step [47]. Also, from this table, it was declared that the Elovich equation does not fit well with the experimental data.

3.2. Sorption mechanisms

It is known that a typical liquid/solid adsorption involves film diffusion, intraparticle diffusion, and mass action. For physical adsorption, mass action is a very rapid process and can be negligible for kinetic study. Thus, the kinetic process

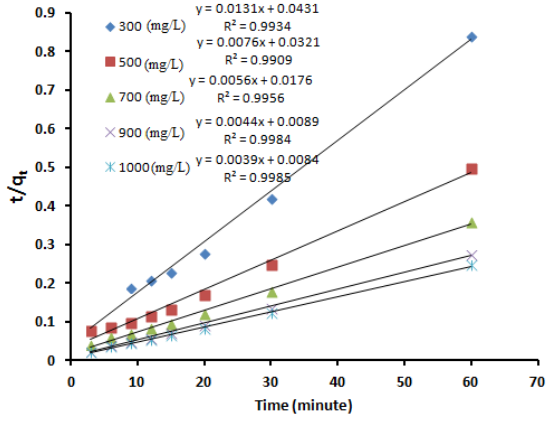

Fig. 3. Second-order plot for chromium (VI) ions removal using AMB.

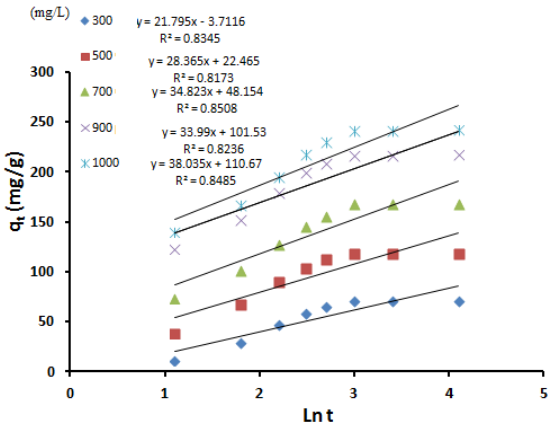

Fig. 4. Simple Elovich plot for chromium (VI) ions removal using AMB.

Table 2
The values of the pseudo-second-order constants

Cr(VI) (mg/L)	R^2	$q_{(calc)}$	$q_{(exp)}$	K_2
300	0.993	76.33	71.2	0.0131
500	0.991	131.57	119	0.0076
700	0.996	178.57	168.6	0.0056
900	0.998	227.3	217.8	0.0044
1,000	0.999	256.4	242.5	0.0039

Table 3
The Elovich model constants

α (mg/g min)	β (g/mg)
3.7116	21.8
22.465	28.37
48.154	34.82
101.53	34
110.53	38

of adsorption is always controlled by liquid film diffusion or intraparticle diffusion, i.e., one of the processes should be the rate-limiting step [48]. Therefore, adsorption diffusion models are mainly constructed to describe the process of film diffusion and intraparticle diffusion. To illuminate the diffusion of Cr(VI) ions through AMB, the diffusion rate equation inside particulate of Dumwald–Wagner and intraparticle models were used to calculate the diffusion rate. On the other hand concerning the external mass transfer, Boyd model was examined to determine the actual rate-controlling step for the Cr(VI) ions adsorption.

The linear plot of Ln $(1 - F^2)$ vs. t indicates the applicability of Dumwald–Wagner kinetic model (Fig. 5). The diffusion rate constants for Cr(VI) ions diffusion inside AMB were tabulated in Table 4.

The intraparticle diffusion plot for Cr(VI) ions adsorption onto AMB was given in Fig. 6. As shown in the figure, the plots were not linear over the whole time range and can be separated into three distinct linear regions. The values of k_d and C were determined from the slopes and intercepts of the linear portions, respectively, that are listed in Table 5. At the initial stage, instantaneous adsorption resulted in the sharper portion of each plot. Although the regressions were linear, these plots did not pass through the origin. Thus, the intraparticle diffusion applied to this system, but it was not the only rate-limiting step during the adsorption. Additional processes, such as the adsorption on the boundary layer, may also be involved in the control of the adsorption rate. The slope of each line was increased with increasing Cr(VI) ions concentration, thereby indicating that a multitude of Cr(VI) ions interacted with the active sites on the adsorbent. Thus, a high adsorption capacity was observed at high Cr(VI) ions concentrations, as shown in Fig. 1. Subsequently, the adsorption decelerated as a consequence of the decreased concentration gradient of Cr(VI) ions between the aqueous and solid phases, as shown by the second linear portion of the curves. Finally, the adsorption reached the equilibrium stage, in which the intraparticle diffusion decreased because of the extremely low Cr(VI) ions concentration in the solution. Meanwhile, the diffusion rate constants of each Cr(VI) ions concentration followed the order of $k_{d1} > k_{d2} > k_{d3}$ (Table 5). The first diffusion stage was the fastest, and the k_{d1} rate constants for the adsorption of Cr(VI) ions were significantly higher than the succeeding rate constants, which might be attributed to the existence of fresh active sites on the surface of the AMB beads. Furthermore, the data in Table 5 illustrate that the intercept C increased with increasing contact time, suggesting an increase in the effect of the boundary layer [49]. The values of C give an idea about the thickness of the boundary layer. The obtained data is in agreement with published data by Zhang et al. [50].

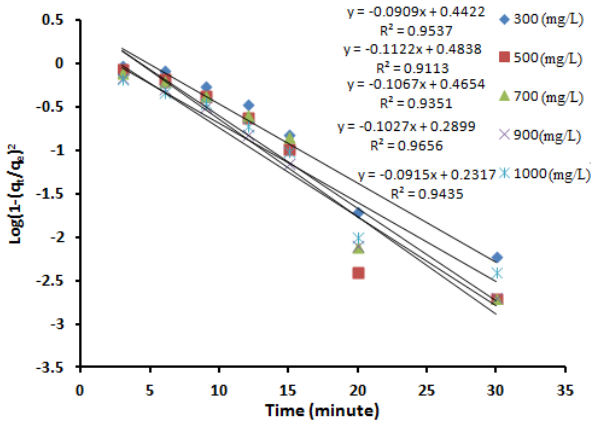

Fig. 5. Dumwald–Wagner plot for chromium (VI) ions removal using AMB.

Table 4
The Dumwald–Wagner diffusion rate constants

Cr(VI) (mg/L)	R^2	K
300	0.9537	0.21
500	0.9113	0.258
700	0.9351	0.246
900	0.9656	0.236
1,000	0.9435	0.217

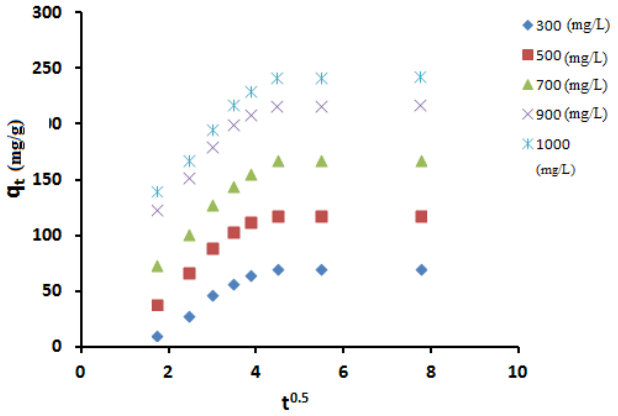

Fig. 6. Intraparticle diffusion plot for chromium (VI) ions removal using AMB.

Table 5
The intraparticle diffusion constants

Cr(VI) (mg/L)	K_{d1}	K_{d2}	K_{d3}	C_1	C_2	C_3	R_1^2	R_2^2	R_3^2
300	28.161	12.339	0.0883	–38.231	15.968	70.516	0.9928	0.9567	1
500	40.333	14.525	0.0442	–33.110	54.535	118.66	1	0.9589	1
700	45.524	22.370	0.0442	–0.8575	68.347	168.26	0.9966	0.9959	1
900	44.107	16.314	0.1325	46.687	144.66	216.77	0.9971	0.9773	1
1,000	43.050	23.164	0.2208	64.467	138.47	240.79	0.9941	0.9809	1

To characterize what the actual rate-controlling step involved in the Cr(VI) ions sorption process, the sorption data were further analyzed by the kinetic expression given by Boyd et al. [37]. The value of B_t can be calculated for each value of F using Eq. (10). The calculated B_t values were plotted against time as shown in Fig. 7. The linearity of this plot will provide useful information to distinguish between external-transport- and intraparticle-transport-controlled rates of sorption. Fig. 7 shows the plot of B_t vs. t, which was a straight line that does not pass through the origin, indicating that film diffusion governs the rate-limiting process [51].

3.3. Sorption isotherm models

Sorption isotherms are mathematical models that describe the distribution of adsorbant species among solid and liquid phases, and they are thus important for chemical design. The results obtained for the sorption of Cr(VI) ions onto AMB were analyzed with the well-known Langmuir, D–R, Freundlich, and Harkins-Jura models. The sorption data obtained for equilibrium conditions were analyzed with the linear forms of these isotherms.

The Langmuir model is valid for monolayer sorption onto a completely homogeneous surface with a finite number of identical sites and with a negligible interaction between adsorbed molecules. According to the R^2 value, which is regarded as a measure of the goodness of fit of experimental data for the isotherm model, the Langmuir equation represents the sorption process of Cr(VI) ions; the R^2 value is 0.7937 (Fig. 8). That indicates not good mathematical fit. The Langmuir parameters for Cr(VI) ions removal, q_m and K, were calculated from the slope and intercept of Fig. 8. The calculated values are 161.3 mg/g and 51.27 L/mg, respectively. That indicates that the AMB was highly efficient for Cr(VI) ions removal and had a moderately high energy of sorption (5.83 L/mg).

On the other hand, the essential characteristics of the Langmuir isotherm are defined by a dimensionless separation factor (R_L) that is indicative of the isotherm shape, which predicts whether an adsorption system is favorable or unfavorable. The calculated values of R_L for Cr(VI) ions removal (Table 6) show favorable adsorption because the R_L values fall between 0 and 1 [52]. This finding, again, confirms that the Langmuir isotherm was favorable for the sorption of Cr(VI) ions onto AMB under the conditions used in this study.

The D–R isotherm is commonly used to describe the sorption isotherms of single solute systems. The D–R isotherm, apart from being an analog of the Langmuir isotherm, is more general than the Langmuir isotherm because it rejects the homogeneous surface or constant adsorption potential. The D–R isotherm model was applied to the equilibrium data obtained from the empirical studies for Cr(VI) ions removal with AMB to determine the nature of the sorption processes (physical or chemical). A plot of Ln q_e against ε^2 is given in Fig. 9. The D–R plot yields a straight line with the R^2 values

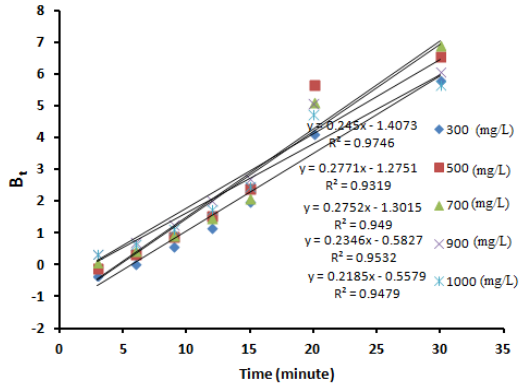

Fig. 7. Boyd expression of the sorption of chromium (VI) ions using AMB.

Table 6
The R_L values for different chromium (VI) ions adsorption using AMB

Cr(VI) (mg/L)	R_L
300	0.000065
500	0.00004
700	0.000028
900	0.000022
1,000	0.00002

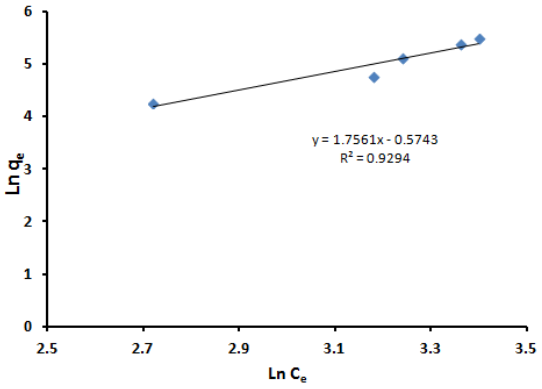

Fig. 8. Langmuir isotherm for the sorption of chromium (VI) ions using AMB.

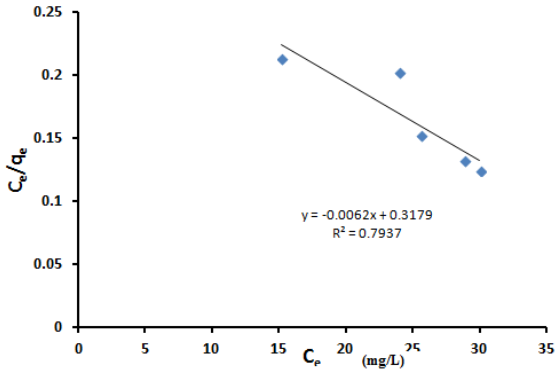

Fig. 9. Freundlich isotherm for the sorption of chromium (VI) ions using AMB.

equal to 0.854, and this indicates that the D–R model less fits the experimental data in comparison with the Freundlich and more fits the experimental data in comparison with the Langmuir isotherm models. According to the plotted D–R isotherm, the model parameters V'_m, K', and E are equal to 302.57 mg/g, 0.0041mol^2/kJ^2, and 0.091kJ/mol, respectively. The calculated adsorption energy ($E < 8$ kJ/mol) indicates that the Cr(VI) ions sorption processes could be considered physisorption in nature [53]. Therefore, it is possible that physical means such as electrostatic forces played a significant role as sorption mechanisms for the sorption of Cr(VI) ions in this work.

The Freundlich isotherm is a widely used equilibrium isotherm model but provides no information on the monolayer sorption capacity, in contrast to the Langmuir model [54,55]. The Freundlich isotherm model assumes neither homogeneous site energies nor limited levels of sorption. The Freundlich model is the earliest known empirical equation and has been shown to be consistent with the exponential distribution of active centers, which is characteristic of heterogeneous surfaces [35]. The values of Freundlich constants, n_f and K_F, estimated from the slope and intercept of the linear plot (Fig. 10) were 0.57 and 0.56, respectively. From the estimated values of n_f, it was found that $n_f < 1$ dictated less favorable sorption for Cr(VI) ions with the AMB beads [56].

The Harkins-Jura isotherm considers the multilayer adsorption and can be explained by the existence of a heterogeneous pore distribution. The model shows the best fit of the results where R^2 value is 0.9852.

Finally, all the R^2 values obtained from the four equilibrium isotherm models applied to Cr(VI) ions sorption on AMB are summarized in Table 7. The Langmuir model R^2 value is 0.7937. This indicates that the adsorbed Cr(VI) ions are not presented as a monolayer sorption, the AMB beads surface is neither completely homogeneous nor with a finite number of identical sites, and the interaction between adsorbed molecules is not negligible. The D–R isotherm, apart from being an analog of the Langmuir isotherm, is more general than the Langmuir isotherm because it rejected the homogeneous surface or constant adsorption potential and used to determine the nature of the sorption processes (physical or chemical). The R^2 value is equal to 0.854, and this indicates that the D–R model more fits the experimental data in comparison with the Langmuir isotherm models. The Freundlich isotherm model assumes nonhomogeneous site energies and multilayers of sorption. The Freundlich model yielded R^2 value (0.9294), and this indicates that the Freundlich model more fits the experimental data in comparison with the Langmuir and D–R model isotherm models. The Harkins-Jura isotherm is analogous to the Freundlich model in addition to considering the existence of a heterogeneous pore distribution. The model shows the best fit of the results where R^2 value is 0.9852 (Fig. 11). The conclusion from the obtained results indicates the formation of multilayers of sorption and the pores nature of the adsorbent. Although the Freundlich model mainly assumes the formation of adsorbate multilayers, the obtained R^2 value (0.9294) was not the best. To validate the Freundlich model, the nonlinear form has been illustrated in Fig. 12. From the figure, it is clear that the R^2 value increased up to 0.9838.

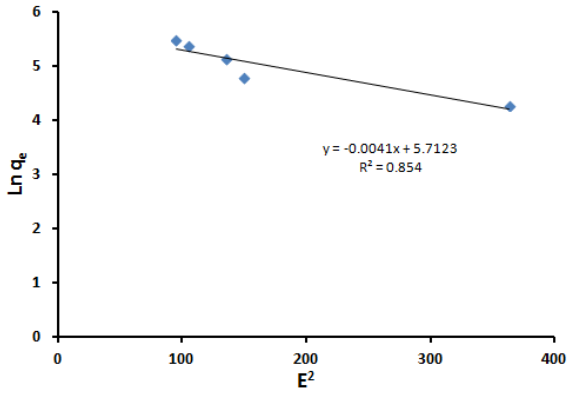

Fig. 10. Dubinin–Radushkevich isotherm for the sorption of chromium (VI) ions using AMB.

Table 7
The R^2 values for chromium (VI) ions removal with the different studied equilibrium isotherms

Isotherm model	R^2
Langmuir	0.7937
Dubinin–Radushkevich	0.854
Freundlich	0.9294 (0.9838)
Harkins-Jura	0.9852

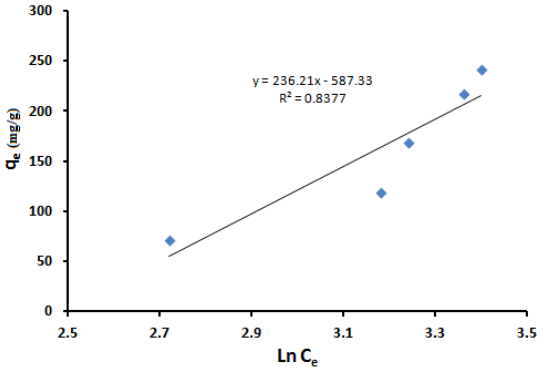

Fig. 11. Harkins-Jura isotherm for the sorption of chromium (VI) ions using AMB.

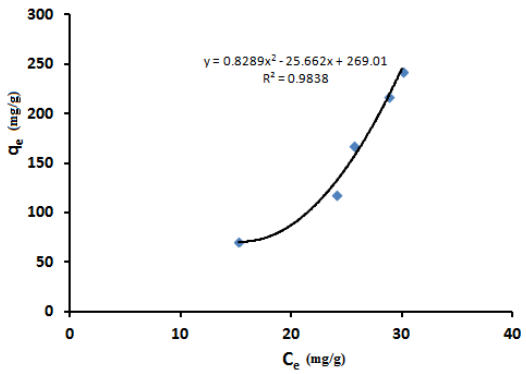

Fig. 12. Freundlich isotherm for the sorption of chromium (VI) ions using AMB (nonlinear form).

4. Conclusion

The bench-scale studies were carried out for the removal of Cr(VI) ions with different initial concentrations using AMB. The kinetics of the Cr(VI) ions sorption rate was best explained by the pseudo-second-order kinetic equation. The Elovich kinetic model confirmed that the ion-exchange mechanism played a significant role in all the studied Cr(VI) ions sorption systems.

Among the four adsorption isotherms tested, the Harkins-Jura and Freundlich models yielded the highest R^2 values: 0.9852 and 0.9838, respectively. That showed the formation of adsorbate multilayers onto nonhomogeneous site energies of AMB beads having heterogeneous pore distribution. The calculated adsorption energy using D–R isotherm (E < 8 kJ/mol) indicates that the Cr(VI) ions sorption processes could be considered physisorptional in nature.

Finally, the diffusion mechanism of Cr(VI) ions was described by different adsorption diffusion models. The intraparticle diffusion was applied to this system, but it was not the only rate-limiting step during the adsorption. Further analyses of the obtained results by the kinetic expression given by Boyd indicate that the film diffusion is the rate-limiting process.

References

[1] E. Merian, Ed., Metals and Their Compounds in the Environment, VCH, Weinheim, Germany, 1991.
[2] E.G. Farmaki, N.S. Thomaidis, Current status of the metal pollution of the environment of Greece - a review, Global NEST J., 10 (2008) 366–375.
[3] Z. Kowalakshi, Treatment of chromic tannery wastes, J. Hazard. Mater., 37 (1994) 137–144.
[4] G. Crini, Recent developments in polysaccharide-based materials used as adsorbents in wastewater treatment, Prog. Polym. Sci., 30 (2005) 38–70.
[5] R. Mehra, M. Juneja, Adverse health effects in workers exposed to trace/toxic metals, Indian J. Biochem. Biophys., 40 (2003) 131–135.
[6] US Department of Health and Human Services, Profile for Chromium, Public Health Service Agency for Toxic substances and Diseases, Washington, DC, 1991.
[7] S.P.B. Kamaludeen, K.R. Arunkumar, S. Avudainayagam, K. Ramasamy, Bioremediation of chromium contaminated environments, Indian J. Exp. Biol., 41 (2003) 972–985.
[8] E. Parameswari, A. Lakshmanan, T. Thilagavathi, Chromate resistance and reduction by bacterial isolates, Aust. J. Basic Appl. Sci., 3 (2009) 1363–1368.
[9] L.S. Clesceri, A.E. Greenberg, A.D. Easton, Eds., Standard Methods for the Examination of Water and Wastewater, 20th ed., Vol. 3, American Public Health Association, 1998, p. 65.
[10] Metcalf, Eddy, Eds., Wastewater Engineering: Treatment of Reuse, 4th ed., McGraw Hill Co., New York, 2003.
[11] Gerard Kiely, Environmental Engineering, McGraw -Hall International Editions, Columbus, OH, USA, 1998.
[12] R.K. Trivedy, Pollution Management in Industries, Environmental Publications, Karad, India, 1979.
[13] S.S. Chen, C.Y. Cheng, C.W. Li, P.H. Chai, Y.M. Chang, Reduction of chromate from electroplating wastewater from pH 1 to 2 using fluidized zero valent iron process, J. Hazard. Mater., 142 (2007) 362–367.
[14] R. Upadhyay, Removal of chromium from electroplating industry waste water, J. Ind. Pollut. Contr., 8 (1992) 81–84.
[15] M.T. Ahmed, S. Taha, T. Chaabane, D. Akretche, R. Maachi, G. Dorange, Nanofiltration process applied to the tannery solutions, Desalination, 200 (2006) 419–420.
[16] B. Preetha, T. Viruthagiri, Bioaccumulation of chromium(VI), copper(II) and nickel(II) ions by growing *Rhizopus arrhizus*, Biochem. Eng. J., 34 (2007) 131–135.
[17] S.A. Cavaco, S. Fernandes, M.M. Quina, L. Ferreira, Removal of chromium from electroplating industry effluent by ion exchange resins, J. Hazard. Mater., 144 (2007) 634–638.
[18] P.A. Kumar, M. Ray, S. Chakraborty, Hexavalent chromium removal from wastewater using aniline formaldehyde condensate coated silica gel, J. Hazard. Mater., 143 (2007) 24–32.
[19] L.T. Arenas, E.C. Lima, A.A. Santos, J.C.P. Vaghetti, T.M.H. Costa, E.V. Benvenutti, Use of statistical design of experiments to evaluate the sorption capacity of 1,4-diazoniabicycle [2.2.2] octane/silica chloride for Cr(VI) adsorption, Colloids Surf., A, 297 (2007) 240–248.
[20] D. Mohan, K.P. Singh, V.K. Singh, Removal of hexavalent chromium from aqueous solution using low-cost activated carbons derived from agricultural waste materials and activated carbon fabric cloth, Ind. Eng. Chem. Res., 44 (2005) 1027–1042.
[21] I. Ali, V.K. Gupta, Advances in water treatment by adsorption technology, Nat. Protoc., 1 (2006) 2661–2667.
[22] I. Ali, The quest for active carbon adsorbent substitutes: inexpensive adsorbents for toxic metal ions removal from wastewater, Sep. Purif. Rev., 39 (2010) 95–171.
[23] M. Vasanthy, M. Sangeetha, R. Kalaiselvi, A comparative study on the chromium removal efficiency of flyash and commercial activated carbon, J. Ind. Pollut. Contr., 20 (2004) 37–44.
[24] C. Covarrubias, R.A.J. Yanez, R. Garcia, M. Angelica, S.D. Barros, P. Arroyo, E.F. Sousa-Aguiar, Removal of chromium(III) from tannery effluents, using a system of packed columns of zeolite and activated carbon, J. Chem. Technol. Biotechnol., 80 (2005) 899–908.
[25] I. Santiago, V.P. Worland, E.R. Cazares, F. Cadena, Adsorption of Hexavalent Chromium onto Tailored Zeolites, Proc. 47th Purdue Industrial Waste Conference, 1995, pp. 669–710.
[26] S. Dahbi, M. Azzi, N. Saib, M. de la Guardia, R. Faure, R. Durand, Removal of trivalent chromium from tannery waste waters using bone charcoal, Anal. Bioanal. Chem., 374 (2002) 540–546.
[27] A.L. Singh, Removal of chromium from waste water with the help of microbes: a review, e-JST 1 (1994) 1–16.
[28] US Patent 3835042 (Sep. 1974), 5000852 (March 1991), and 7105087 (Sep. 2006); Great Britain: 11394909 (Sep. 1975); Switzerland: 575347 (March 1976); France: 2192071 (Nov. 1976); Canada: 1026472 (Feb 1978).
[29] S. Lagergren, B.K. Svenska, Zur theorie der sogenannten adsorption geloester stoffe, Veternskapsakad Handlingar (Veternskapsakad Documents), 24 (1898) 1–39.
[30] Y.S. Ho, G. McKay, The kinetics of sorption of basic dyes from aqueous solutions by sphagnum moss peat, Can. J. Chem. Eng., 76 (1998) 822–827.
[31] M. Ozacar, I.A. Sengil, A kinetic study of metal complex dye sorption onto pine sawdust, Process Biochem., 40 (2005) 565–572.
[32] G. McKay, M.S. Otterburn, J.A. Aja, Fuller's earth and fired clay as adsorbents for dye stuffs, Water, Air, Soil, Pollut., 24 (1985) 307–322.
[33] W.J. Weber, J.C. Morris, J. Sanity, Kinetics of adsorption on carbon from solution, Eng. Div. Am. Soc. Civil Eng., 89 (1963) 31–59.
[34] M. Sarkar, P.K. Acharya, B. Bhaskar, Modeling the adsorption kinetics of some priority organic pollutants in water from diffusion and activation energy parameters, J. Colloid Interface Sci., 266 (2003) 28–32.
[35] Y.S. Ho, Effect of pH on lead removal from water using tree fern as the sorbent, Bioresour. Technol., 96 (2005) 1292–1996.
[36] N. Unlu, M. Ersoz, Removal characteristics of heavy metal ions onto a low cost biopolymeric sorbents from aqueous solution, J. Hazard. Mater., 136 (2006) 272–280.
[37] G.E. Boyd, A.W. Adamson, I.S. Myers, The exchange adsorption of ions from aqueous solutions by organic zeolites; kinetics, J. Am. Chem. Soc., 69 (1947) 2836–2848.
[38] A. Mohammad, A.K.R. Rifaqat, A. Rais, A. Jameel, Adsorption studies on *Citrus reticulata* (fruit peel of orange): removal and recovery of Ni(II) from electroplating wastewater, J. Hazard. Mater., 79 (2000) 117–131.
[39] I.A.W. Tan, A.L. Ahmad, B.H. Hameed, Adsorption of basic dye using activated carbon prepared from oil palm shell: batch and fixed bed studies, Desalination, 225 (2008) 13–28.

[40] A. Seker, T. Shahwan, A.E. Eroglu, Y. Sinan, Z. Demirel, M.C. Dalay, Equilibrium, thermodynamic and kinetic studies for the biosorption of aqueous lead(II), cadmium(II) and nickel(II) ions on *Spirulina platensis*, J. Hazard. Mater., 154 (2008) 973–980.
[41] M.J. Temkin, V. Pyzhev, Kinetics of Ammonia Synthesis on Promoted Iron Catalysts, Acta Physicochim. URSS, 12 (1940) 327–352.
[42] A.U. Itodo, H.U. Itodo, Sorption energies estimation using Dubinin-Radushkevich and Temkin adsorption isotherms, Life Sci. J., 7 (2010) 31–39.
[43] J. Kota, Z. Stasicka, Chromium occurrence in the environment and methods of its speciation. Environ. Pollut., 107 (2000) 263–283.
[44] J. Jachuła, Z. Hubicki, Removal of Cr(VI) and As(V) ions from aqueous solutions by polyacrylate and polystyrene anion exchange resins, Appl. Water Sci., 3 (2013) 653–664.
[45] T. Shi, Z. Wang, Y. Liu, S. Jia, D. Changming, Removal of hexavalent chromium from aqueous solutions by D301, D314 and D354 anion-exchange resins, J. Hazard. Mater., 161 (2009) 900–906.
[46] Y.S. Ho, G. McKay, Pseudo-second order model for sorption processes, Process Biochem., 34 (1999) 451–465.
[47] R.L. Tseng, Mesopore control of high surface area NaOH-activated carbon, J. Colloid Interface Sci., 303 (2006) 494–502.
[48] F.W. Meng, Study on a Mathematical Model in Predicting Breakthrough Curves of Fixed-Bed Adsorption onto Resin Adsorbent, MS Thesis, Nanjing University, China, 2005, pp. 28–36.
[49] B.K. Nandi, A. Goswami, M.K. Purkait, Adsorption characteristics of brilliant green dye on kaolin, J. Hazard. Mater., 161 (2009) 387–395.
[50] L. Zhang, P. Hu, J. Wang, Q. Liu, R. Huang, Adsorption of methyl orange (MO) by Zr (IV)-immobilized cross-linked chitosan/bentonite composite, Int. J. Biol. Macromolec., 81 (2015) 818–827.
[51] A.E. Ofomaja, Kinetic study and sorption mechanism of methylene blue and methyl violet onto mansonia (*Mansonia altissima*) wood sawdust, Chem. Eng. J., 143 (2008) 85–95.
[52] Y.S. Ho, J.F. Porter, G. McKay, Equilibrium isotherm studies for the sorption of divalent metal ions onto peat: copper, nickel and lead single component systems, Water, Air, Soil, Pollut., 141 (2002) 1–33.
[53] J.M. Smith, Chemical Engineering Kinetics, McGraw-Hill, New York, 1981.
[54] F. Gode, E. Pehlivan, A comparative study of two chelating ion-exchange resins for the removal of chromium(III) from aqueous solution, J. Hazard. Mater., 100 (2003) 231–243.
[55] F. Gode, E. Pehlivan, Adsorption of Cr(III) ions by Turkish brown coals, Fuel Process. Technol., 86 (2005) 875–884.
[56] M.M. Dubinin, E.D. Zaverina, L.V. Radushkevich, Sorption and structure of activated carbons. 1. Investigation of organic vapour adsorption, Zh Fiz Khim, 21 (1947) 1351–1362.